Petroleum and Coal

Article **Open Access**

Parametric Study of Enhanced Condensate Recovery of Gas Condensate Reservoirs using Design of Experiment

Nkemakolam Izuwa, Basil C Ogbunude

Department of Petroleum Engineering; Federal University of Technology, Owerri; Peace Wokoma; University of Port Harcourt. Email: basilogbunude@yahoo.com

Received November 26, 2015; Accepted December 29, 2015

Abstract

Gas condensate reservoirs usually exhibit reduced well productivity because of condensate dropout that occurs below the dew point pressure. Gas recycling has become one of the most favorable methods of improving recovery of condensed liquid. However, understanding the influence of different injection and reservoir parameters on productivity is of great importance when planning a gas recycling scheme. Traditional methods of sensitization during reservoir simulation for gas condensate fields creates the challenge of quick identification of the most critical properties for sensitization, and hence delay of overall simulation project delivery. This work aims at identifying the key variables that influence productivity of a gas condensate reservoir under a gas recycling scheme using the design of experiment approach (DOE). DOE represents a more effective method for computer-enhanced, systematic approach to experimentation, considering all the factors simultaneously. Identification of these parameters will help simulators achieve best optimization targets and also save time and resources during dynamic simulation projects. Furthermore, it will be shown that experimental design can be used to fit responses (condensate/gas production) to mathematical models that will be able to predict outputs for any given combination of variables.

Keywords: Gas condensate; Gas recycling; Design of Experiments.

1. Introduction

Rich gas or retrograde condensate gas reservoir is a common type of hydrocarbon reservoir around the world. Much of the 6,183 trillion cubic feet of worldwide gas reserves can be found in gas condensate reservoirs [1]. Hence, gas condensate reservoirs are important to today's energy demand/supply challenges. On the other hand, gas condensate systems have been recognized as the reservoir type with the most complex flow behavior and thermodynamic characteristics [2].

The gas condensate systems exist as a single-phase fluid (gas) at original reservoir conditions, but unlike a wet or dry gas reservoir, it separates into two phases, a gas and a liquid (condensate) at pressures below the saturation pressure of the reservoir [3]. The main problems associated with gas condensate systems are the formation damage effects leading to a reduced relative permeability of gas because of liquid condensate dropout, and permanent loss of valuable liquid due to the trapping capillary effects in the reservoir [4].

Historically, there are three main methods for gas condensate recovery [5]: natural pressure depletion to the abandonment pressure, full pressure maintenances by gas cycling and partial pressure maintenance by means of gas cycling after previous natural depletion. In order to reduce the impact of the condensate accumulations near the wellbore, gas cycling is usually employed to prevent liquid condensation and to also vaporize dropped out liquid [6]. In properly optimizing recovery from this type of reservoir system, a key question arises to the timing of initiating the gas injection project, as well as understanding the effects of different parameters on the recovery potential of the injection. Though gas-recycling will always improve recovery, there is a need to identify the set of parameters that will lead to a maximum recovery when optimized. Traditional simulation techniques involve testing one factor at a time (OFAT) while holding other factors constant. This work shows how the design of experiments can prove to be a cost-effective way to provide information about the inter-action of variables and the way the whole reservoir system works while displaying how inter-connected factors respond over a wide range of values without requiring direct testing of all possible values. Finally, the design of experiment will be used to develop a system-specific mathematical model that can be used to study the reservoir behaviors based on optimal statistical interactions of the responses (condensate/gas production) and variables (production/ reservoir/injection properties).

2. Methodology

Generally, injection of gas into the reservoir results in an increase in production [7]. However, to obtain optimum productivity, different production and injection conditions are required to be sensitized. Such conditions include the injection pressure, injection rate, and the various reservoir and fluid properties. For the purpose of this study, two reservoir models were used create a dynamic simulation model which was used (together with the reservoir, injection and production variables) as input for the design of experiment.

One of the models is the fluid model which was designed using a set of real fluid data obtained from a Niger Delta retrograde gas field. The other model comprises the bulk reservoir, including its petrophysical properties which were hypothetically designed within the confines of Niger Delta reservoir characteristics.

2.1. Fluid characterization and generation of compositional PVT tables

The fluid properties including the phase behavior are greatly dependent on the properties of each component or pseudo-component and composition [8]. The Peng-Robinson (PR) equation of state (EOS) was applied to design the fluid behavioral patterns at different reservoir temperatures and pressures. The results of this design were compared to the laboratory generated results gotten through various routine tests like constant composition expansion (CCE) and constant volume depletion (CVD). Discrepancies in the two models were adjusted by applying heptane-plus characterization techniques and EOS tuning methods. The heavier components (heptane-plus) have various isomers for the same carbon number components and hence they have different characteristics by the presence of different isomers [9]. The heptane-plus characterization involved splitting into three fractions; C7+, C14+ and C25+ before lumping into groups of all pseudo-components according to their molecular weights. The first pseudo-component GRP1 is composed of carbon dioxide only as the only significant non-hydrocarbon. The second pseudo-gas contains nitrogen, methane, and ethane. The amount of nitrogen is not significant; hence, it is assumed that this pseudo-component contains only methane and ethane. The third pseudo-component contains the gasolines; propane, butanes, pentanes, and hexanes. The fourth group is C7 to C13, while the fifth is C14 to C24. The final group is the heaviest, C25+ components.

Table 1 Composition of pseudo-components

Components	Mol %	Weight fraction, %
GRP1	3.35	6.7572
GRP2	90.69	70.112
GRP3	3.69	9.1893
GRP4	1.9992	11.142
GRP5	0.26079	2.6309
GRP6	0.010017	0.16876

The EOS tuning method applied was the 3-Parameter PR model which involved multiple non-linear regression techniques. After several regressions, the fluid was able to be matched. The parameters used to validate the match are shown in figures 2 – 6.

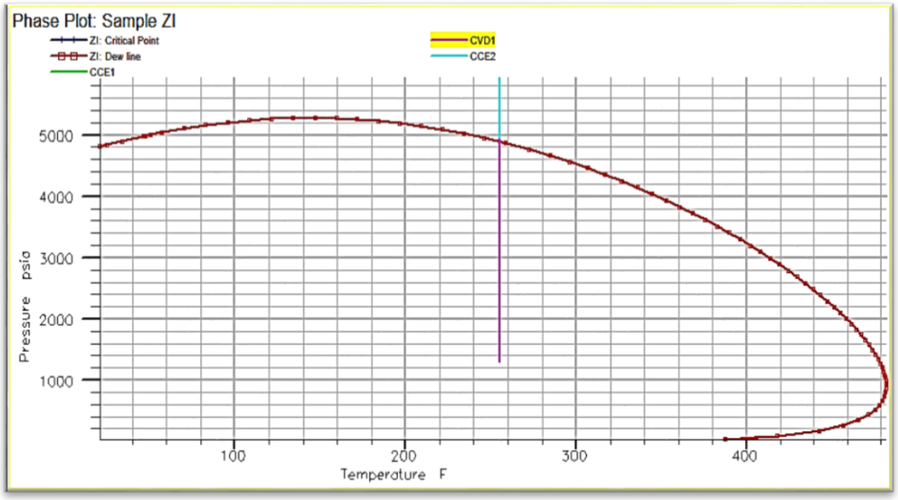

Figure 1 Phase envelope for the gas condensate sample; T_r =255^{O}F, P_i =4953psia

```
Expt DEW1   : Retrograde Dew Point Pressure Calculation

Peng-Robinson          (3-Parm)  on ZI       with PR corr.
Lohrenz-Bray-Clark Viscosity Correlation

Specified temperature            Deg F              255.0000
Calculated dew point pressure    PSIA              4768.9919
Observed   dew point pressure    PSIA              4769.0000

-------------------  ------------ ------------
                        Liquid       Vapour
Fluid properties     ------------ ------------
                      Calculated   Calculated
-------------------  ------------ ------------
Mole Weight               92.8731      21.8187
Z-factor                   1.3365       1.0068
Viscosity                  0.4032       0.0271
Density    LB/FT3         43.2098      13.4764
Molar Vol  CF/LB-ML        2.1494       1.6190
-------------------  ------------ ------------
```

Figure 2 Result of saturation pressure EOS tuning showing the matched dew point pressure

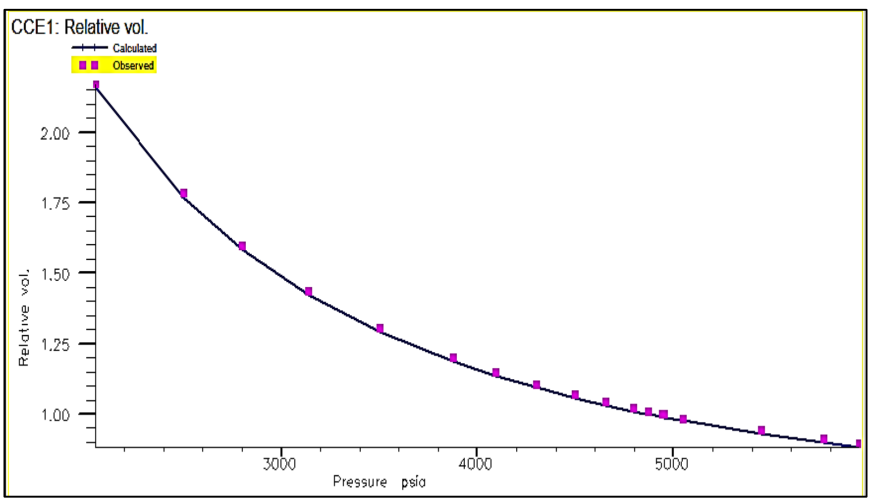

Figure 3 Experimental and calculated relative volume for CCE @ 255^{O}F

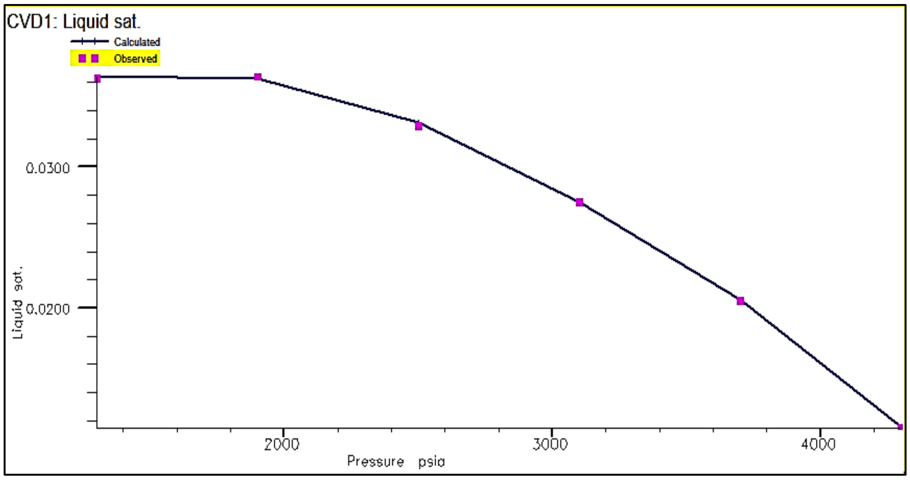

Figure 4 Experimental and calculated liquid saturation for CVD @ 225 ^{o}F

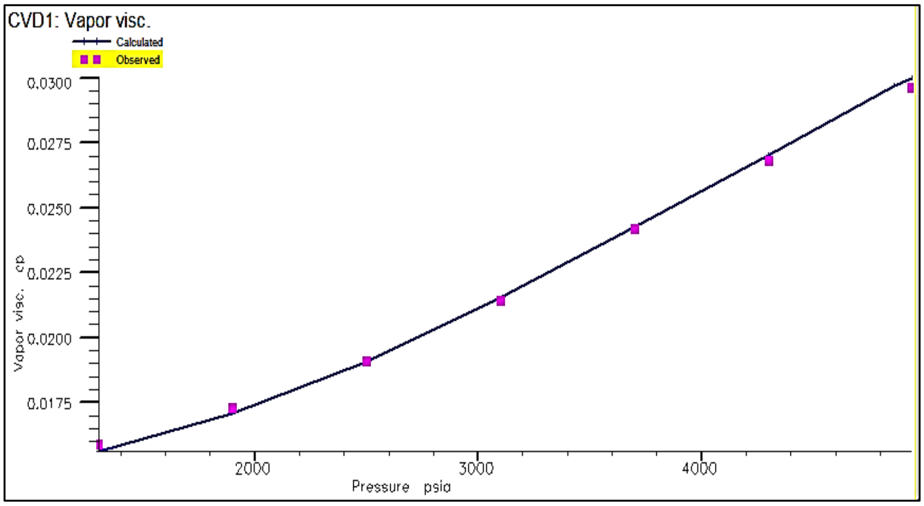

Figure 5 Experimental and calculated gas viscosity for CVD @ 255 ^{o}F

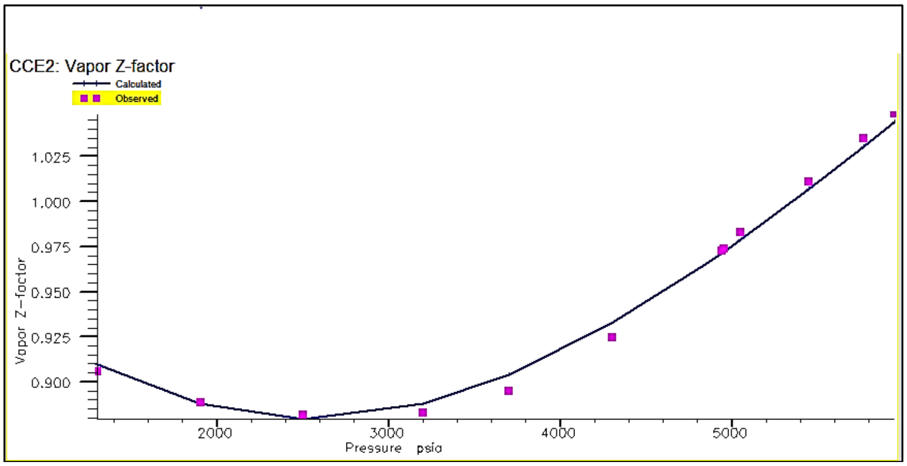

Figure 6 Experimental and calculated gas compressibility factor data for CVD @ 255 ^{o}F

2.2. Reservoir model and experimental design

A simple five-spot model was designed using hypothetical grid blocks, rock properties and initialization properties. The synthetic model has Cartesian coordinates with block-centered geometry having length of 328 ft. in the X and Y directions with 10x10x7 grids. The reservoir which was at a depth of 9560 ft. below sea level has an initial reservoir pressure of 4953 psia. Figure 7 below shows the 3D block model of the synthetic reservoir showing the 4 producing flank wells (P_1, P_2, P_3, P_4) and a single gas recycling/injection well (I) at the center.

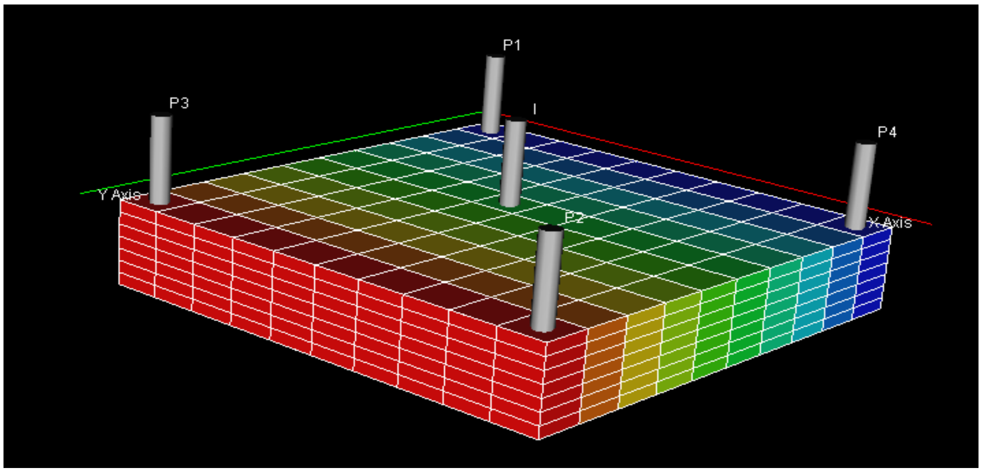

Figure 7 3D simulation model of reservoir

Sensitivity analyses are common during reservoir simulations. To understand the prevailing factors that are most contributory to the final responses in the dynamic modeling of a gas recycling project in a gas condensate reservoir, the DOE technique was applied. In this method, eleven properties expected to influence gas and condensate production are taken as factors to be used in the experimental design procedure and thus determine the statistical effects of these different parameters on gas and condensate recovery. Responses are the condensate and gas production, generated for each combination of parameters. DOE provides information about the interactions of the factors and responses and how interconnected factors respond over a wide range of values, without the need to test all possible values directly. The Plackett-Burman DOE Design for selection of significant parameters was used for the eleven factors (parameters), where each factor was varied over two levels (low and high) based on regional petrophysical and operational characteristic

Table 2 Plackett-Burman Design showing the factors and levels (Low and High)

Factor	Name	Unit	Low	High
A	PORO	fraction	0.1	0.38
B	PERM	mD	100	1000
C	NTG	fraction	0.4	0.9
D	Kv/Kh	fraction	0.01	0.1
E	Scc	fraction	0.1	0.4
F	CGR	stb/scf	50	240
G	Qinj	scf/day	2480	24800
H	Pinj	psia	1400	7000
J	H	ft.	40	200
K	Pr	psia	3000	7000
L	Krg	fraction	0.2	0.85

Table 3 Experimental design table showing the factors and responses used for the design

	Factor 1	Factor 2	Factor 3	Factor 4	Facto r 5	Factor 6	Factor 7	Factor 8	Factor 9	Factor 10	Factor 11	Response 1	Response 2
Run	A:PORO fraction	B:PERM mD	C:NTG fraction	D:Kv/Kh fraction	E:Scc fraction	F:CGR stb/scf	G:Qinj scf/day	H:Pinj psia	J:H ft.	K:Pr psia	L:Krg fraction	Gas Prod Mscf	Cond Prod bbls
1	0.38	100	0.9	0.1	0.1	240	24800	7000	40	3000	0.2	135780000	1113184.1
2	0.1	1000	0.4	0.1	0.4	50	24800	7000	200	3000	0.2	135780000	747511.69
3	0.1	100	0.4	0.01	0.1	50	2480	1400	40	3000	0.2	2242552.8	51224.289
4	0.38	100	0.9	0.1	0.4	50	2480	1400	200	3000	0.85	95895064	2225145.8
5	0.1	100	0.9	0.01	0.4	240	2480	7000	200	7000	0.2	52022840	1503648
6	0.38	1000	0.9	0.01	0.1	50	24800	1400	200	7000	0.2	135780000	4400179
7	0.1	1000	0.9	0.01	0.4	240	24800	1400	40	3000	0.85	135780000	212694.67
8	0.1	1000	0.9	0.1	0.1	50	2480	7000	40	7000	0.85	9727697	276220.78
9	0.38	1000	0.4	0.1	0.4	240	2480	1400	40	7000	0.2	15023919	425837.5
10	0.38	100	0.4	0.01	0.4	50	24800	7000	40	7000	0.85	135780000	1034212.6
11	0.1	100	0.4	0.1	0.1	240	24800	1400	200	7000	0.85	85265984	196071.72
12	0.38	1000	0.4	0.01	0.1	240	2480	7000	200	3000	0.85	4651961	101806.91

This generates a set of saturated screening designs based on Plackett-Burman structures, the number of factors being one less than the number of required runs. These runs are a mixture of the different levels of the factors as shown in table 3.

3. Results

With the results of the design, the various levels of significance of the eleven parameters on gas and condensate production responses were observed using the normal probability plot and the Pareto chart. Interpretation of the charts gave rise to identification of seven factors that showed the most significant impact on the production responses.

These parameters are

- Porosity
- Net-to-Gross ratio
- Kv/Kh
- Injection Rate
- Injection Pressure
- Thickness
- Reservoir Pressure

These parameters were chosen based on the analyses of the results of the Plackett-Burman design as shown in figures 8, 9 and 10.

The normal probability plot is a plot of the ordered values of the normal percentage probability versus the expected standardized effects from the simulation results. The parameters having an effect on the responses appear as outliers of the straight line. The ones with a negative effect are shown to the left of the line while the parameters with positive influence are shown to the right of the line. Those on the line have very little or no significant effect on the responses.

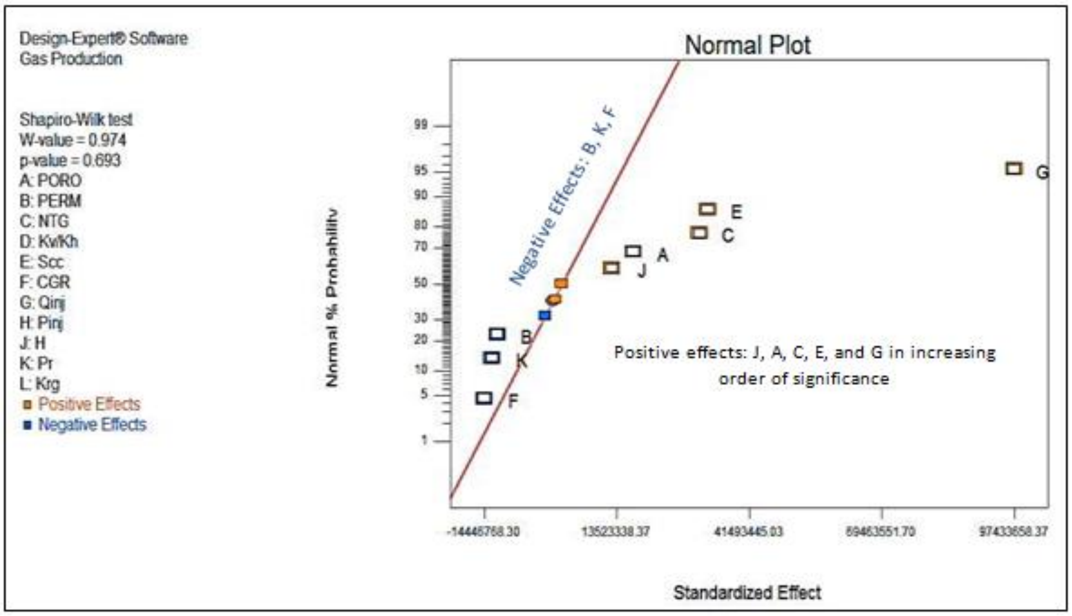

Figure 8 Graph of normal % probability vs. standardized effects for gas production

The Pareto chart displays the t values of the effects and the effects above the Bonferroni line show certainty of significance for the parameter, giving a more comfortable viewing for the selection of significant effects. The seven parameters were selected based on weighting of the effects derived from the Pareto Charts and Normal Plots for the gas and condensate models.

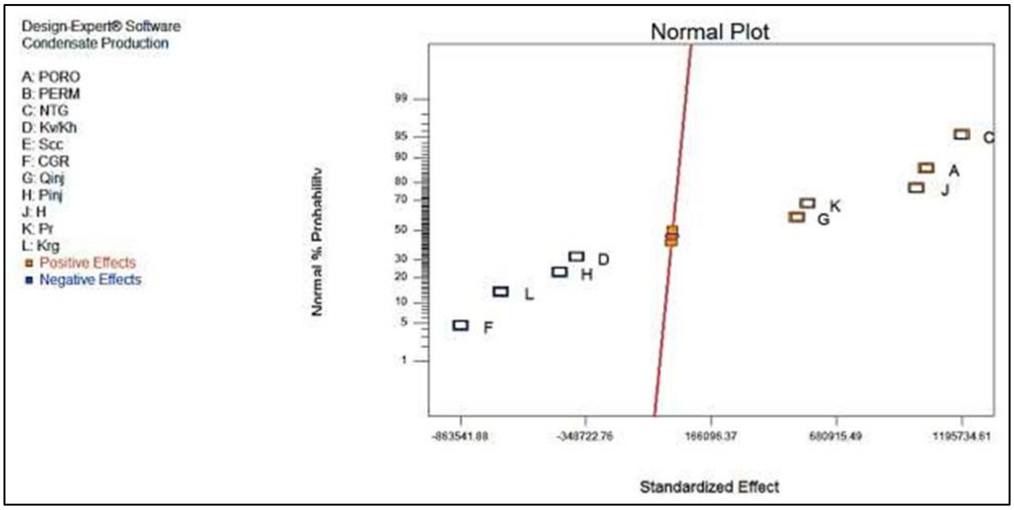

Figure 9 Graph of normal % probability vs. standardized effects for condensate production

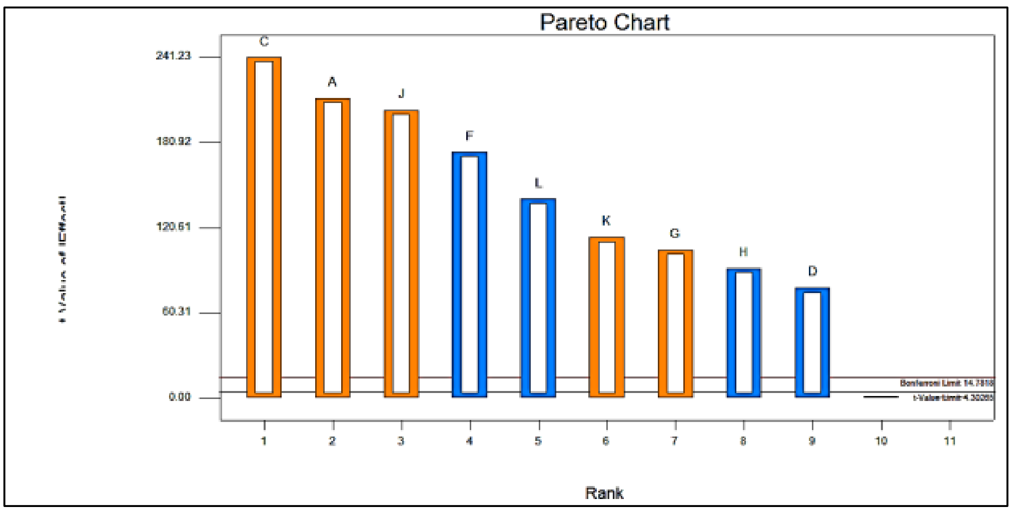

Figure 10(a) Pareto chart for cond prod, showing factor C as the most significant parameter

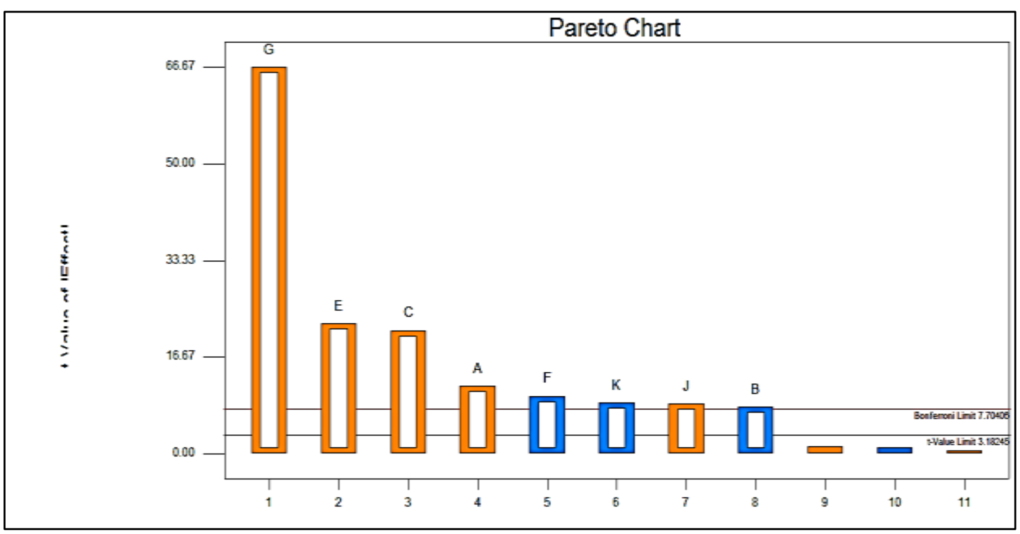

Figure 10(b) Pareto chart for gas prod., showing G as the most significant parameter

3.1. Development of proxy

As an extension to the work, a mathematical model was developed using D-optimal Response Surface Method (RSM) to study the effects of these factors on gas and condensate recovery. RSM designs help to quantify the relationships between one or more measured responses and the vital input factors or parameters. The D-optimal criteria is one of the optimalities that selects design points in a way that minimizes the variance associated with the estimates of specified model coefficients. The aim is to generate a model that represents the responses using quadratic interactions of the factors. Using the quadratic model, an overall candidate point set was created, after which fifty –five specific design points (the experimental runs that would be done) were chosen after which the proxy was generated.

This proxy was tested using statistical indicators to ascertain its degree of error as shown in tables 4 and 5 for gas and condensate production respectively.

Table 4 Statistical summary for gas prediction model

Indicator	Value	Indicator	Value
Std. Dev.	-	R-Squared	0.987586
Mean	81063030	Adj R-Squared	0.964719
C.V. %	12.75986	Pred R-Squared	0.822069
PRESS	2.91E+16	Adeq Precision	20.91767

Table 5: Statistical summary for condensate prediction model

Indicator	Value	Indicator	Value
Std. Dev.	-	R-Squared	0.994997
Mean	1352464	Adj R-Squared	0.98578
C.V. %	10.06817	Pred R-Squared	0.934002
PRESS	4.65E+12	Adeq Precision	40.23579

At the end of the experimental design, the following equations were generated for the gas and condensate production;

$$\begin{aligned}\boldsymbol{G_p}, C_P =\ & A_1 + A_2(\emptyset) + A_3\,(NTG) + A_4\,({}^{K_V}/_{K_H}) + A_5\,(Q_{inj}) + A_6\,(H) + A_7\,(P_r) + A_8\,(P_{inj}) \\ & + A_9\,(\emptyset * NTG) + A_{10}\left(\emptyset * {}^{K_V}/_{K_H}\right) + A_{11}\,(\emptyset * Q_{\text{inj}}) + A_{12}\,(\emptyset * H) + A_{13}\,(\emptyset * P_r) \\ & + A_{14}\,(\emptyset * P_{inj}) + A_{15}\left(NTG * {}^{K_V}/_{K_H}\right) + A_{16}\,(NTG * Q_{inj}) + A_{17}\,(NTG * H) \\ & + A_{18}\,(NTG * P_r) + A_{19}\,(NTG * P_{inj}) + A_{20}\left({}^{K_V}/_{K_H} * Q_{inj}\right) + A_{21}\left({}^{K_V}/_{K_H} * H\right) \\ & + A_{22}\left({}^{K_V}/_{K_H} * P_r\right) + A_{23}\left({}^{K_V}/_{K_H} * P_{inj}\right) + A_{24}(Q_{inj} * H) + A_{25}(Q_{inj} * P_r) \\ & + A_{26}(Q_{inj} * P_{inj}) + A_{27}(H * P_r) + A_{28}\,(H * P_{inj}) + A_{29}(P_r * P_{inj}) + A_{30}(\emptyset^2) + A_{31}(NTG^2) \\ & + A_{32}\left[\left({}^{K_V}/_{K_H}\right)^2\right] + A_{33}(Q_{inj}{}^2) + A_{34}(H^2) + A_{35}(P_r{}^2) + A_{36}(P_{inj}{}^2)\end{aligned}$$

The values of the coefficients for gas and condensate equations are represented in table 6.

The mathematical model was validated by comparing them to results generated from an independent dynamic simulator. For the gas production model, the relative error when compared to simulation results was found to be 3.8 %, while that for condensate production prediction model was 3.6%.

Finally, a sensitivity analysis was carried out on these parameters using the mathematical models to help understand how these factors influence production in a gas condensate reservoir.

Table 6 Coefficients of gas and condensate equation

Constants	Coefficients	
	Gas production	Condensate production
A_1	$4.60738*10^7$	$1.04572*10^6$
A_2	$-5.30696*10^7$	$-4.41239*10^6$
A_3	$-1.35533*10^8$	$-3.74945*10^6$
A_4	$-7.34830*10^7$	$2.43062*10^6$
A_5	1176.33385	51.19948
A_6	$4.49593*10^5$	-4815.17296
A_7	-7244.68379	-15.93230
A_8	-9111.02877	-25.52929
A_9	$1.56111*10^8$	$4.7435*10^6$
A_{10}	$5.30660*10^8$	$1.5562*10^6$
A_{11}	-6257.17754	11.78361
A_{12}	$7.33963*10^5$	33198.09102
A_{13}	-2228.53531	630.74498
A_{14}	13414.38501	12.50100
A_{15}	$-2.22378*10^8$	$-3.20724*10^6$
A_{16}	-2319.93384	-7.00348
A_{17}	$3.29370*10^5$	10852.73623
A_{18}	4522.62490	143.36173
A_{19}	-208.50250	-22.02281
A_{20}	5071.25296	40.98690
A_{21}	-78705.33842	3950.85908
A_{22}	7658.12602	-72.92741
A_{23}	33312.15701	335.85908
A_{24}	-14.36637	0.048639
A_{25}	-0.25318	$-2.87403*10^{-3}$
A_{26}	$3.33435*10^{-3}$	0.000000
A_{27}	42.58720	1.43811
A_{28}	29.45486	0.074765
A_{29}	1.22107	$7.49886*10^{-3}$
A_{30}	$8.03938*10^6$	$-3.59965*10^6$
A_{31}	$7.70745*10^7$	$1.84886*10^6$
A_{32}	$7.13256*10^8$	$-1.52469*10^7$
A_{33}	0.31962	$-7.03805*10^{-4}$
A_{34}	-3031.83758	-35.35163
A_{35}	0.13735	-0.017308
A_{36}	-0.80404	$-1.94740*10^{-3}$

3.2. Effects of injection rate and pressure on gas and condensate production

Five injection rates were chosen for the injection process ranging from 19,800 Mscf/day to 5,900 Mscf/day, and the effects of each rate on gas and condensate production was ana-lyzed. It can be seen from the graphs above that the maximum gas production occurs at the maximum injection rate. This also coincides with the maximum injection pressure. However, the lowest injection rate, 5,900 Mscf/day does not give the lowest cumulative gas production. Generally, the optimum injection rate will always depend on the prevailing economic conditions of the operating environment.

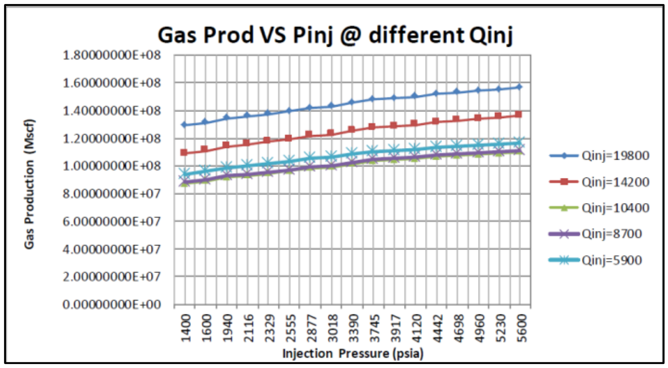

Figure 11 Effects of injection rate and pressure on gas production

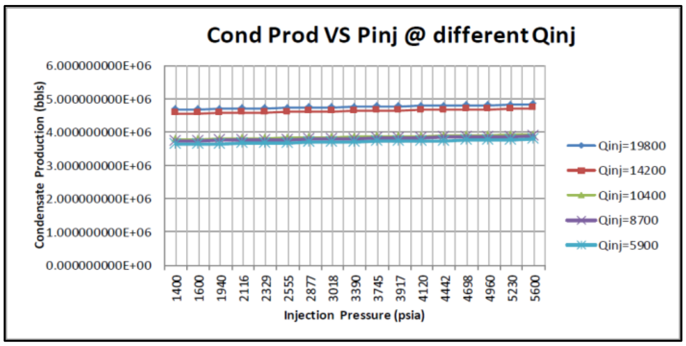

Figure 12 Effects of injection rate and pressure on condensate production

3.3. Effects of permeability ratio on gas and condensate production

For this parameter, the sensitivity was done at different injection rates. This was aimed at studying the possible existing of interaction between the two parameters for both gas and condensate production and to confirm if the little changes in condensate production observed with increasing injection pressure observed in figure 12 was particular to injection rates only.

The permeability ratio does not have a lot of variation on gas production, especially at very low injection rate. However, the effect of permeability ratio on condensate production is very pronounced when correlated with injection pressure, as seen in Figures 13f-j. At very high injection rates and injection pressures, the highest permeability ratio (Kv/Kh = 0.1) gives the maximum condensate production while at very low injection rates and injection pressures.

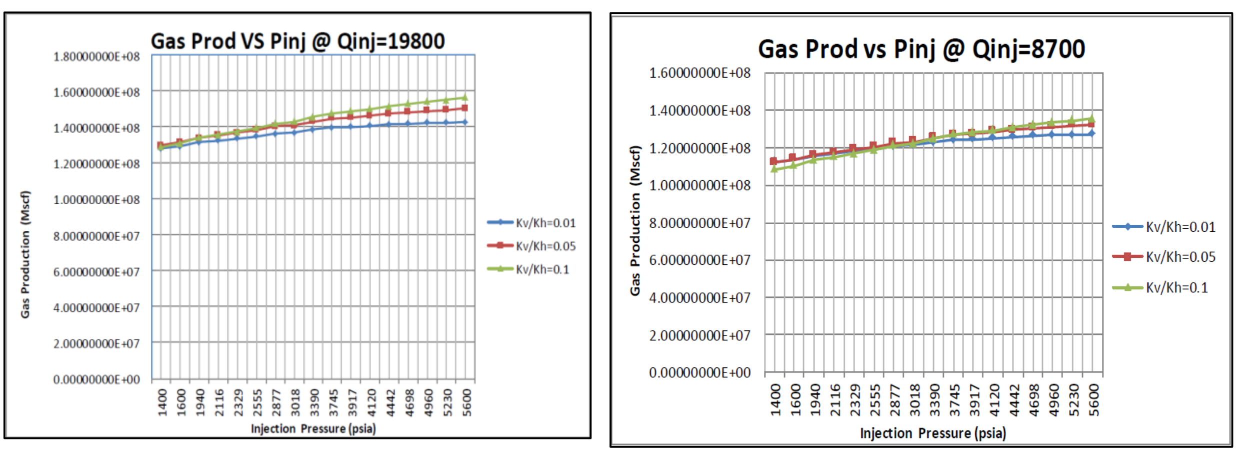

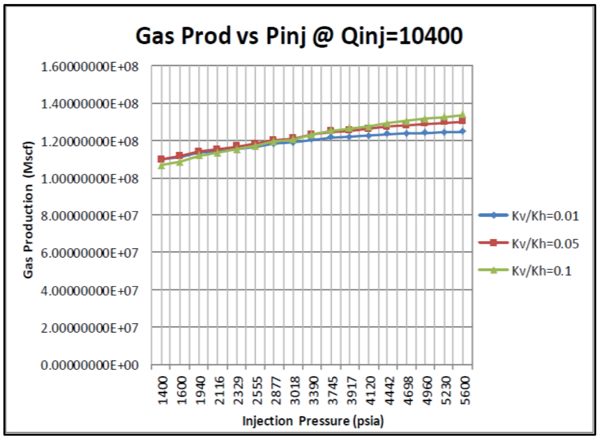
Gas Prod vs Pinj @ Qinj=10400
Gas Production (Mscf)
1.60000000E+08
1.40000000E+08
1.20000000E+08
1.00000000E+08
8.00000000E+07
6.00000000E+07
4.00000000E+07
2.00000000E+07
0.00000000E+00
1400 1600 1940 2116 2329 2555 2877 3018 3390 3745 3917 4120 4442 4698 4960 5230 5600
Injection Pressure (psia)
Kv/Kh=0.01
Kv/Kh=0.05
Kv/Kh=0.1

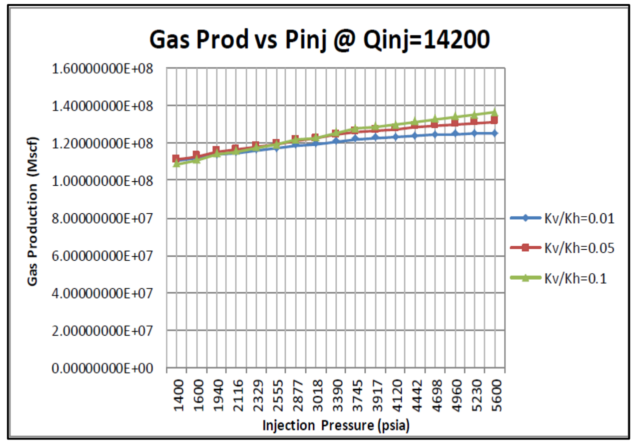
Gas Prod vs Pinj @ Qinj=14200
Gas Production (Mscf)
1.60000000E+08
1.40000000E+08
1.20000000E+08
1.00000000E+08
8.00000000E+07
6.00000000E+07
4.00000000E+07
2.00000000E+07
0.00000000E+00
1400 1600 1940 2116 2329 2555 2877 3018 3390 3745 3917 4120 4442 4698 4960 5230 5600
Injection Pressure (psia)
Kv/Kh=0.01
Kv/Kh=0.05
Kv/Kh=0.1

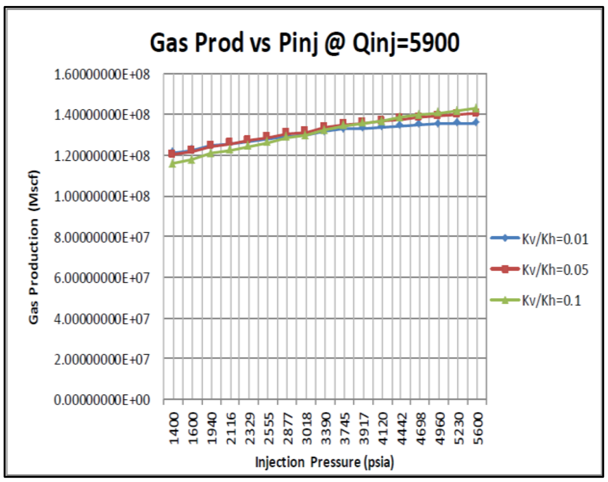
Gas Prod vs Pinj @ Qinj=5900
Gas Production (Mscf)
1.60000000E+08
1.40000000E+08
1.20000000E+08
1.00000000E+08
8.00000000E+07
6.00000000E+07
4.00000000E+07
2.00000000E+07
0.00000000E+00
1400 1600 1940 2116 2329 2555 2877 3018 3390 3745 3917 4120 4442 4698 4960 5230 5600
Injection Pressure (psia)
Kv/Kh=0.01
Kv/Kh=0.05
Kv/Kh=0.1

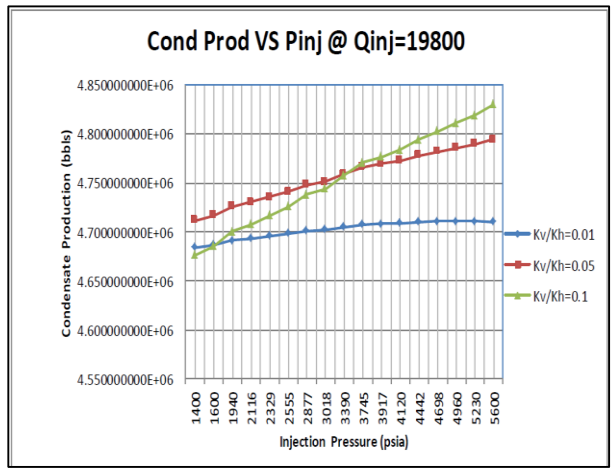
Cond Prod VS Pinj @ Qinj=19800
Condensate Production (bbls)
4.850000000E+06
4.800000000E+06
4.750000000E+06
4.700000000E+06
4.650000000E+06
4.600000000E+06
4.550000000E+06
1400 1600 1940 2116 2329 2555 2877 3018 3390 3745 3917 4120 4442 4698 4960 5230 5600
Injection Pressure (psia)
Kv/Kh=0.01
Kv/Kh=0.05
Kv/Kh=0.1

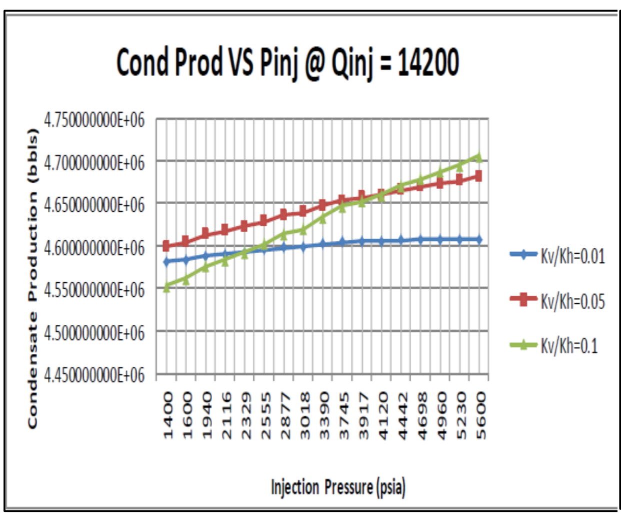
Cond Prod VS Pinj @ Qinj = 14200
Condensate Production (bbls)
4.750000000E+06
4.700000000E+06
4.650000000E+06
4.600000000E+06
4.550000000E+06
4.500000000E+06
4.450000000E+06
1400 1600 1940 2116 2329 2555 2877 3018 3390 3745 3917 4120 4442 4698 4960 5230 5600
Injection Pressure (psia)
Kv/Kh=0.01
Kv/Kh=0.05
Kv/Kh=0.1

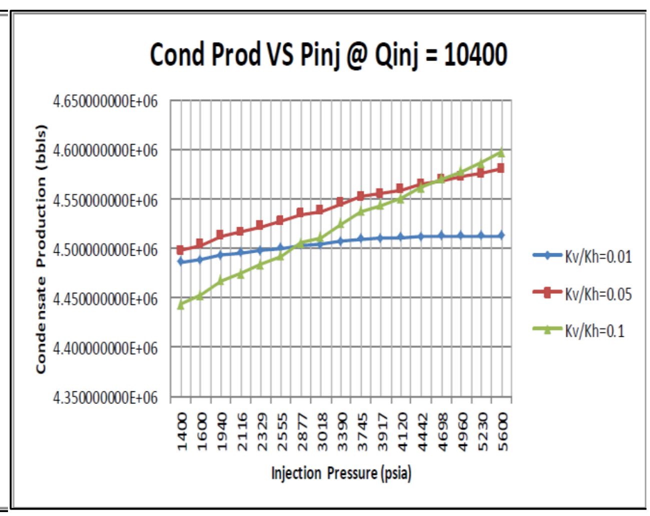
Cond Prod VS Pinj @ Qinj = 10400
Condensate Production (bbls)
4.650000000E+06
4.600000000E+06
4.550000000E+06
4.500000000E+06
4.450000000E+06
4.400000000E+06
4.350000000E+06
1400 1600 1940 2116 2329 2555 2877 3018 3390 3745 3917 4120 4442 4698 4960 5230 5600
Injection Pressure (psia)
Kv/Kh=0.01
Kv/Kh=0.05
Kv/Kh=0.1

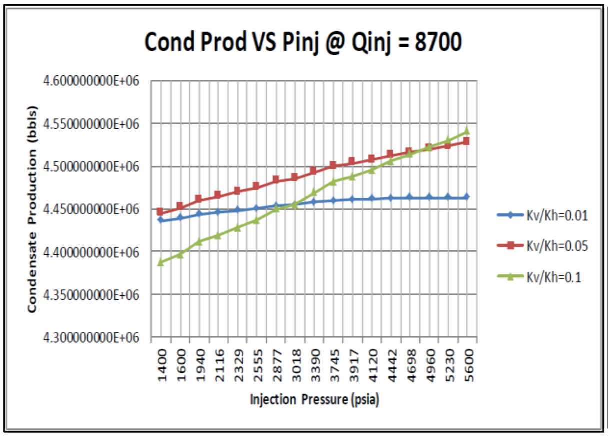

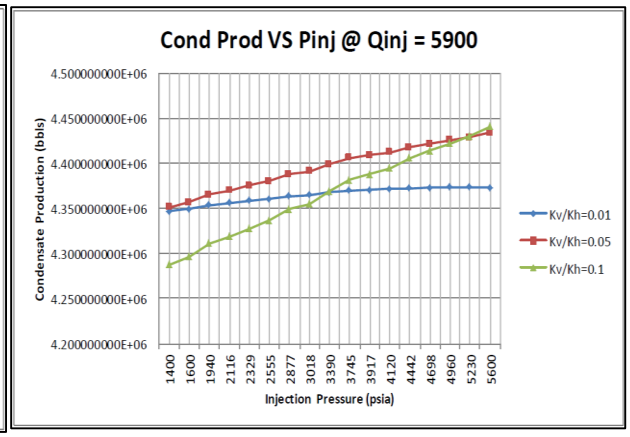

Figures 13a-j effects of different permeability ratios on gas and cond. production at different injection rates

3.4. Effects of Net-to-Gross ratio on gas and condensate production

Both gas and condensate production showed similar effects with NTG sensitivity (Figures 14 and 15). As expected, higher values of NTG gave lower responses of productivity.

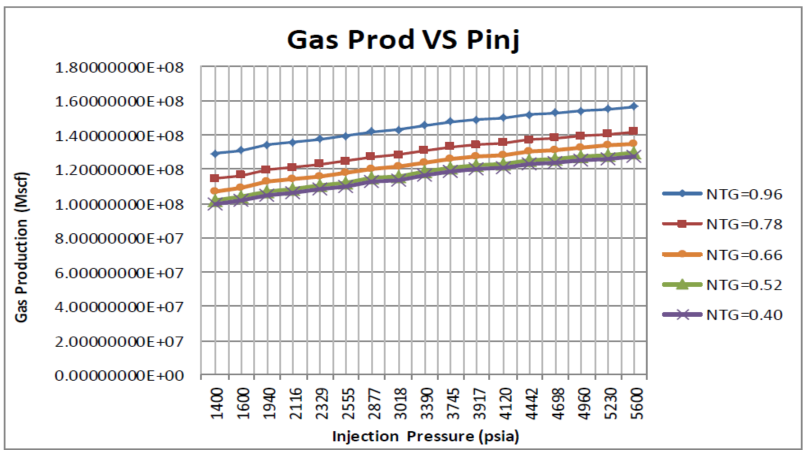

Figure 14 Effects of Net-to-Gross ratio on gas production

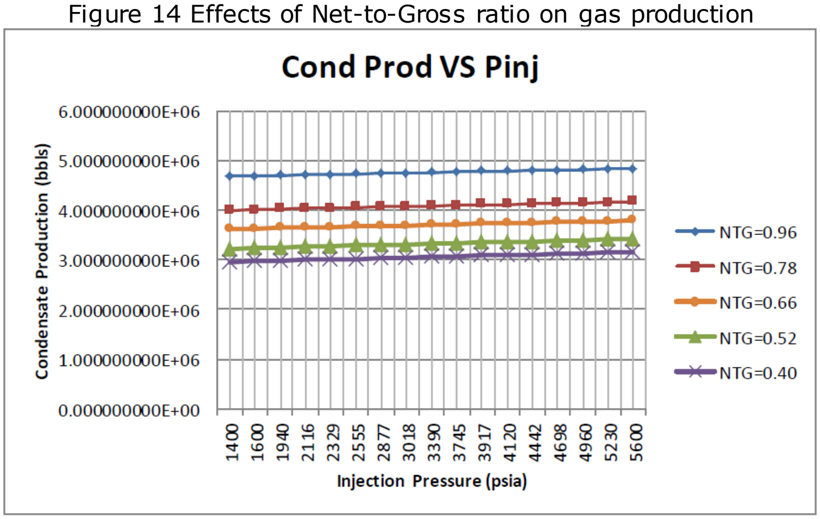

Figure 15 Effects of Net-to-Gross ratio on condensate production

3.5. Effects of porosity on gas and condensate production

For this sensitivity, the porosity was correlated with different injection rates to study their effects on gas and condensate production (Figures 16 and 17). As expected, the least production occurs in the least porous system. However, the least gas production for each given porosity system does not coincide with the lowest injection rate. A similar observation was also made when studying the effects of injection rate at different injection pressures (Figure 11). Again, this shows that economic conditions could influence the nature of the outcome of the sensitivity involving injection rates. Similar observations were made in the condensate analysis.

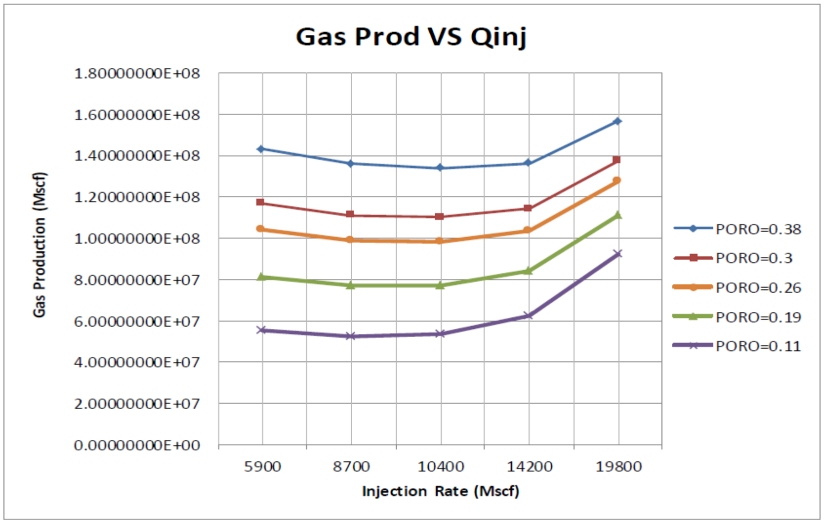

Figure16 Effects of porosity on gas production at varying injection rates

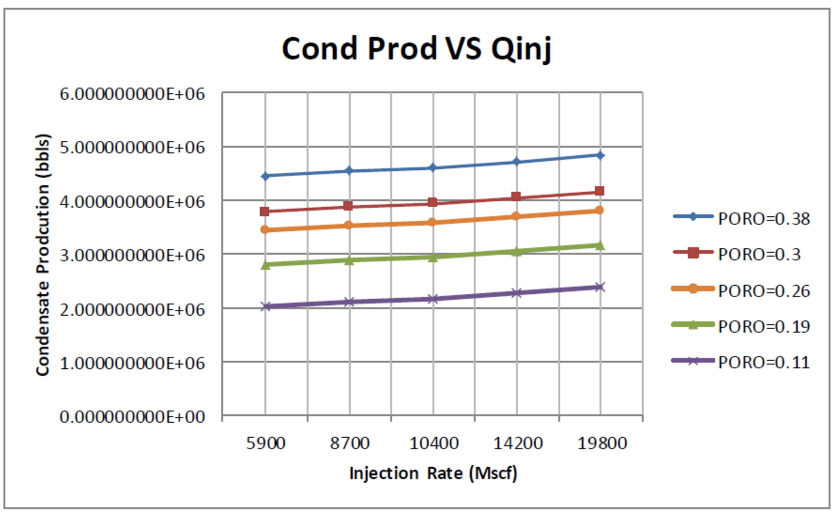

Figure17 Effects of porosity on condensate production at varying injection rates

3.6. Effects of gross thickness on gas and condensate production at varying porosity

Using an NTG of 0.96, the thickness was sensitized on at different porosity. At high porosity, it is observes that the maximum production coincides with the highest thickness. However, as the porosity decreases, this fails to hold. At the lowest porosity system of 0.11, it is obser-ved that the highest gas production does not coincide with the highest thickness of 200 ft. All the above hold true for the condensate production, except that even at low porosity systems, the maximum production still coincides with the maximum thickness of 200 ft.

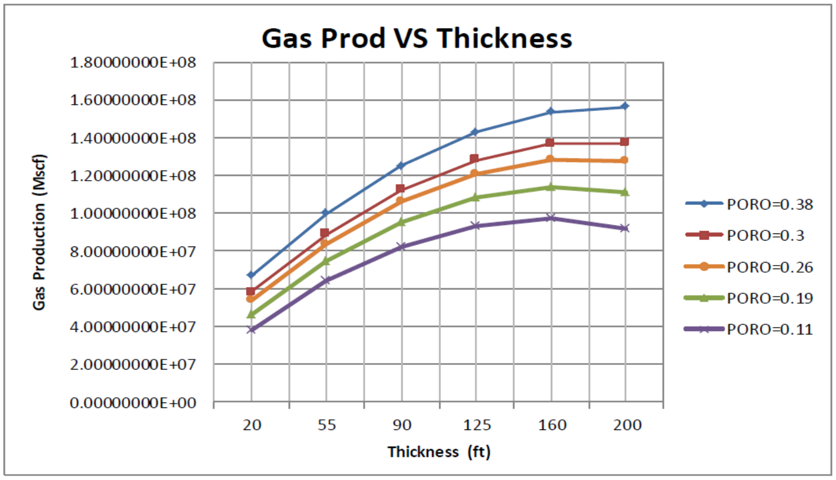

Figure 18 Effects of thickness on gas production at varying porosity values

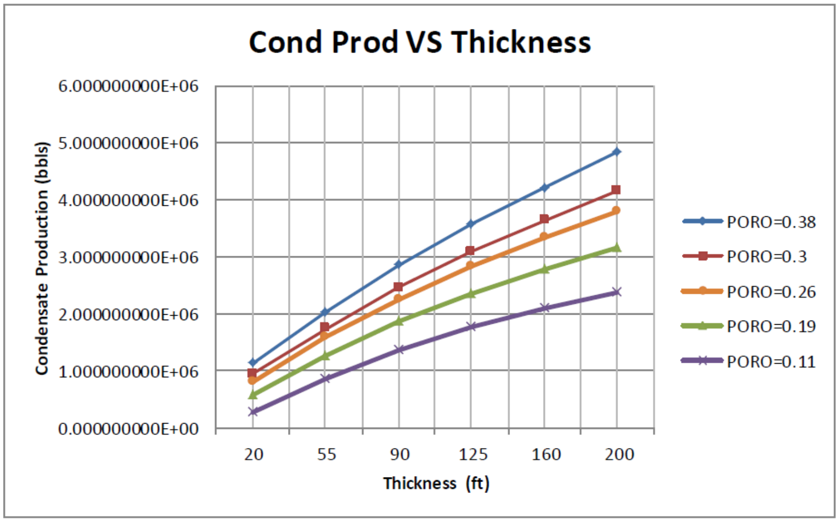

Figure 19 Effects of thickness on condensate production at varying porosity values

4. Conclusion

Gas condensate reservoirs are known to be very valuable because of the condensate's high API (American Petroleum Institute) value. Producing this fluid however has been met with several challenges over the years. This is abated by injection of produced gas into the formation to evaporate the condensed fluid. Due to the sensitive nature of this kind of reservoir, it is very important to understand the parameters that influence production, and know how these parameters influence production. This work proposed a hypothetical model that was used to study the effects of different parameters on gas and condensate production through statistical optimization. It was discovered that several parameters did affect production of reservoir fluids under varying conditions more than others.

References

[1] Nathan M, Hadi N, Ding Z. Application of Horizontal Wells to Reduce Condensate Blockage in Gas Condensate Reservoirs. Paper SPE 130996 presented at CPS/SPE International Oil and Gas Conference and Exhibition2010, Beijing, China.

[2] Chunmei S. Flow Behavior of Gas Condensate Wells. A Dissertation Submitted to the Department of Energy Resources Engineering2009, Stanford University, California, USA.

[3] Barnum RS, Brinkman FP, Richardson TW and Spillette,AG. Gas Condensate Reservoir Behavior: Productivity and Recovery Reduction due to Condensation 1995, Paper SPE 30767.

[4] Fevang O. and Whitson CH. Modeling Gas Condensate Well Deliverability, Paper SPE 30714 presented at the 1995 SPE Annual Technical conference and Exhibition, Dallas.

[5] Henderson GD, Danesh A, Trehran DH, and Peden JM. An Investigation Governing the Flow and Recovery in Different Flow Regimes Present in Gas Condensate Reservoirs, Paper SPE 26661, presented at the 1993 Annual Technical Conference and Exhibition, Houston, Texas.

[5] Carlson, M.R. and Myer, J.W.G (1999), "Reduced Productivity Impairment for Fracture Stimulated Gas Condensate Wells", JCPT, 1999, Vol. 38, No. 13.

[6] Douglas EK and Behie GA. Third SPE Comparative Solution Project: Gas Cycling of Retrograde Condensate Reservoirs. Paper SPE 12278, JPT 1987.

[7] Bourbiaux B. Parametric study of Gas condensate Reservoir Behavior during Depletion: A Guide for Development planning, Paper SPE 28848, presented at the 1994 EUROPEC, London.

[8] Danesh, A., Henderson, G.D., Krinis, D., and Peden, J.M. (1988), "Experimental Investigation of Retrograde Condensation in Porous Media at Reservoir Conditions", Paper SPE 18316

[9] Whitson CH, Torp SB. Evaluating Constant –Volume Depletion Data, J.Pet. Tech. (March 1983): 610-20.

[10] Anderson M. Design of Experiments, The Industrial Physicist, American Institute of Physics.

[11] Tarek A, Evans J, Kwan R and Vivian T. Wellbore liquid blockage in gas condensate reservoirs. Paper SPE 51050, Presented at the 1998 SPE Eastern Regional meeting, Pittsburgh.